

Production of the Smallest QED Atom: True Muonium ($\mu^+ \mu^-$)

Stanley J. Brodsky*

SLAC National Accelerator Laboratory, Stanford University, Stanford, California 94309, USA

Richard F. Lebed†

Department of Physics, Arizona State University, Tempe, Arizona 85287-1504, USA

(Received 22 April 2009; published 26 May 2009)

The “true muonium” ($\mu^+ \mu^-$) and “true tauonium” ($\tau^+ \tau^-$) bound states are not only the heaviest, but also the most compact pure QED systems. The rapid weak decay of the τ makes the observation of true tauonium difficult. However, as we show, the production and study of true muonium is possible at modern electron-positron colliders.

DOI: 10.1103/PhysRevLett.102.213401

PACS numbers: 36.10.Ee, 12.20.Ds, 13.66.De, 31.30.jr

The possibility of a $\mu^+ \mu^-$ bound state, denoted here as ($\mu^+ \mu^-$), was surely realized not long after the clarification [1] of the leptonic nature of the muon, since the first positronium calculations [2] and its observation [3] occurred in the same era. The term “muonium” for the $\mu^+ e^-$ bound state and its first theoretical discussion appeared in Ref. [4], and the state was discovered soon thereafter [5]. However, the first detailed studies [6,7] of ($\mu^+ \mu^-$) (alternately dubbed “true muonium” [7] and “dimuonium” [8,9]) only began as experimental advances made its production tenable. Positronium, muonium, $\pi\mu$ atoms [10], and more recently even dipositronium [the ($e^+ e^-$)($e^+ e^-$) molecule] [11] have been produced and studied, but true muonium has not yet been produced.

The true muonium ($\mu^+ \mu^-$) and true tauonium ($\tau^+ \tau^-$) [and the much more difficult to produce “mu-tauonium” ($\mu^\pm \tau^\pm$)] bound states are not only the heaviest, but also the most compact pure QED systems [the ($\mu^+ \mu^-$) Bohr radius is 512 fm]. The relatively rapid weak decay of the τ unfortunately makes the observation and study of true tauonium more difficult, as quantified below. In the case of true muonium the proposed production mechanisms include $\pi^- p \rightarrow (\mu^+ \mu^-) n$ [6], $\gamma Z \rightarrow (\mu^+ \mu^-) Z$ [6], $e Z \rightarrow e(\mu^+ \mu^-) Z$ [12], $Z_1 Z_2 \rightarrow Z_1 Z_2 (\mu^+ \mu^-)$ [13] (where Z indicates a heavy nucleus), direct $\mu^+ \mu^-$ collisions [7], $\eta \rightarrow (\mu^+ \mu^-) \gamma$ [14], and $e^+ e^- \rightarrow (\mu^+ \mu^-)$ [15]. In addition, the properties of true muonium have been studied in a number of papers [9,16,17].

The $e^+ e^- \rightarrow (\mu^+ \mu^-)$ production mechanism is particularly interesting because it contains no hadrons, whose concomitant decays would need to be disentangled in the reconstruction process. If the beam energies of the collider are set near threshold $\sqrt{s} \sim 2m_\mu$, the typical beam spread is so large compared to bound-state energy level spacings that every nS state is produced, with relative probability $\sim 1/n^3$ [i.e., scaling with the ($\mu^+ \mu^-$) squared wave functions $|\psi_{n00}(0)|^2$ at the interaction point, $r = 0$] and carrying the Bohr binding energy $-m_\mu \alpha^2/4n^2$. The high- n

states are so densely spaced that the total cross section is indistinguishable [18] from the rate just above threshold, after including the Sommerfeld-Schwinger-Sakharov (SSS) threshold enhancement factor [19] from Coulomb rescattering. As discussed below [Eq. (2) and following], the SSS correction $\sim \pi\alpha/\beta$ cancels the factor of β , the velocity of either of μ^\pm in their common center-of-momentum (c.m.) frame, that arises from phase space.

The spectrum and decay channels for true muonium are summarized in Fig. 1, using well-known quantum mechanical expressions [20] collected in Table I. In most cases, the spectrum and decay widths of ($\mu^+ \mu^-$) mimic the spectrum of positronium scaled by the mass ratio m_μ/m_e . However, while positronium of course has no $e^+ e^-$ decay channels, ($\mu^+ \mu^-$)[$n^3 S_1$] $\rightarrow \gamma^* \rightarrow e^+ e^-$ is allowed and has a rate and precision spectroscopy sensitive to vacuum polarization corrections via the timelike running coupling $\alpha(q^2 > 0)$.

Unlike in the case of positronium, the ($\mu^+ \mu^-$) constituents themselves are unstable. However, the μ has an

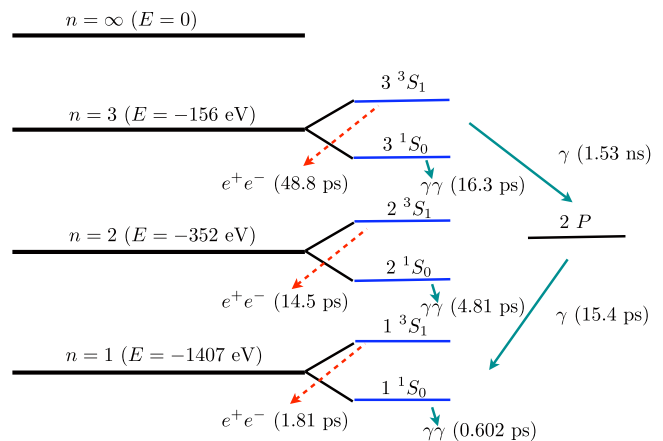


FIG. 1 (color online). True muonium level diagram (spacings not to scale).

TABLE I. True fermionium decay times and their ratios.

$\tau(n^3S_1 \rightarrow e^+e^-) = \frac{6\hbar n^3}{\alpha^3 mc^2},$	$\tau(n^1S_0 \rightarrow \gamma\gamma) = \frac{2\hbar n^3}{\alpha^3 mc^2},$
$\tau(2P \rightarrow 1S) = \left(\frac{3}{2}\right)^8 \frac{2\hbar}{\alpha^3 mc^2},$	$\tau(3S \rightarrow 2P) = \left(\frac{5}{2}\right)^9 \frac{4\hbar}{3\alpha^3 mc^2},$
$\frac{\tau(n^3S_1 \rightarrow e^+e^-)}{\tau(n^1S_0 \rightarrow \gamma\gamma)} = 3,$	$\frac{\tau(2P \rightarrow 1S)}{\tau(n^1S_0 \rightarrow \gamma\gamma)} = \left(\frac{3}{2}\right)^8 \frac{1}{n^3} = \frac{25.6}{n^3},$
$\frac{\tau(3S \rightarrow 2P)}{\tau(2P \rightarrow 1S)} = \left(\frac{5}{3}\right)^9 = 99.2.$	

exceptionally long lifetime by particle physics standards (2.2 μ s), meaning that $(\mu^+\mu^-)$ annihilates long before its constituents weakly decay, and thus true muonium is unique as the heaviest metastable laboratory possible for precision QED tests: $(\mu^+\mu^-)$ has a lifetime of 0.602 ps in the 1S_0 state (decaying to $\gamma\gamma$) [6,7] and 1.81 ps in the 3S_1 state (decaying to e^+e^-) [6].

In principle, the creation of true tauonium ($\tau^+\tau^-$) is also possible; the corresponding 1S_0 and 3S_1 lifetimes are 35.8 and 107 fs, respectively, to be compared with the free τ lifetime 291 fs (or half this for a system of two τ 's). One sees that the $(\tau^+\tau^-)$ annihilation decay and the weak decay of the constituent τ 's actually compete, making $(\tau^+\tau^-)$ not a pure QED system like (e^+e^-) .

Electron-positron colliders have reached exceptional luminosity values, leading to the possibility of detecting processes with very small branching fractions. The original proposal by Moffat [15] suggested searching for x rays from $(\mu^+\mu^-)$ Bohr transitions such as $2P \rightarrow 1S$ at directions normal to the beam. However, the nS states typically decay via annihilation to e^+e^- and $\gamma\gamma$ before they can populate longer-lived states. Furthermore, the production and rapid decay of a single neutral system at rest or moving in the beam line would be difficult to detect relative to the continuum QED backgrounds, due to a preponderance of noninteracting beam particles and synchrotron radiation.

In this Letter we propose two distinct methods for producing a moving true muonium atom in e^+e^- collisions. In both methods the motion of the atom allows one to observe a gap between the production point at the beam crossing and its decay to e^+e^- or $\gamma\gamma$ final states. Furthermore, each given lifetime is enhanced by a relativistic dilation factor γ appropriate to the process.

In the first method, we utilize an e^+e^- collider in which the atomic system produced in $e^+e^- \rightarrow \gamma^* \rightarrow (\mu^+\mu^-)$ at $s \simeq 4m_\mu^2$ carries momentum $\vec{p} = \vec{p}_{e^+} + \vec{p}_{e^-} \neq 0$. The production point of the $(\mu^+\mu^-)$ and its decay point are thus spatially displaced along the beam direction. Asymmetric e^+e^- colliders PEP-II and KEKB have been utilized for the BABAR and Belle experiments. However, we propose configuring an e^+e^- collider to use the ‘‘Fool’s Intersection Storage Ring’’ (FISR) discussed by Bjorken [21] (Fig. 2) in which the e^\pm beams are arranged to merge at a small angle 2θ (bisected by \hat{z}), so that $s = (p_{e^+} + p_{e^-})^2 \simeq 2E_+E_-(1 - \cos 2\theta) \simeq 4m_\mu^2$ and the atom moves with momentum $p_z = (E_+ + E_-)\cos\theta$. For example, for $\theta = 5^\circ$ and equal-energy e^\pm beams $E_\pm = 1.212$ GeV, the atom has lab-frame momentum $p_z = 2.415$ GeV and $\gamma =$

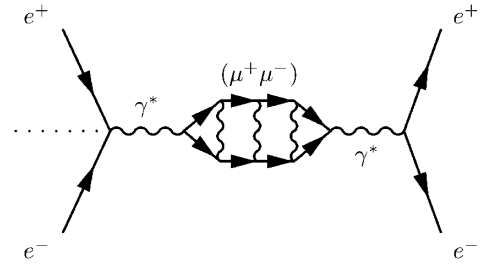


FIG. 2. The ‘‘Fool’s ISR’’ configuration for $e^+e^- \rightarrow (\mu^+\mu^-)$ for symmetric beam energies. The angle between either of the e^\pm and dotted line (\hat{z} axis) is defined as θ .

$E_{\text{lab}}/2m_\mu = 11.5$. One can thus utilize symmetric or asymmetric beams in the GeV range colliding at small angles to obtain the c.m. energy $\sqrt{s} \simeq 2m_\mu$ for the production of true muonium.

The gap between the formation of the atom and its decay as it propagates should be clearly detectable since its path lies in neither beam pipe. The 3S_1 state decays with a 50 ps lifetime, so it moves 1.5 cm of proper distance before decaying to e^+e^- , a length enhanced in the lab frame by the γ factor (to 16.8 cm in the $\theta = 5^\circ$ example). One can thus observe the appearance of e^+e^- events with a θ -dependent set of lifetimes.

The cross section for continuum muon pair production $e^+e^- \rightarrow \mu^+\mu^-$ just above threshold is the Born cross section enhanced by the SSS threshold Coulomb resummation factor [19] $S(\beta)$:

$$\sigma = \frac{2\pi\alpha^2\beta}{s} \left(1 - \frac{\beta^2}{3}\right) S(\beta), \quad (1)$$

where

$$S(\beta) = \frac{X(\beta)}{1 - \exp[-X(\beta)]}. \quad (2)$$

Here $\beta = \sqrt{1 - 4m_\mu^2/s}$ is the velocity of either of the μ^\pm in their c.m. frame, and $X(\beta) = \pi\alpha\sqrt{1 - \beta^2}/\beta$. Thus the factor of β due to phase space is canceled by the SSS factor, so that continuum production occurs even at threshold where $\beta = 0$. For values of $|\beta|$ of order α (as in Bohr bound states), we see that the SSS factor effectively replaces β with $\pi\alpha$. Below threshold the entire set of ortho-true muonium n^3S_1 , $C = -$ Bohr bound-state resonances with $n = 1, 2, \dots$ is produced, with weights $\sim 1/n^3$ and spaced with increasing density according to the Bohr energies $(\sqrt{s})_n \simeq 2m_\mu - \alpha^2 m_\mu / 4n^2$. By duality, the rates smeared over energies above and below threshold should be indistinguishable [18]. Thus the total production of bound states in $e^+e^- \rightarrow (\mu^+\mu^-)$ relative to the $e^+e^- \rightarrow \mu^+\mu^-$ relativistic lepton pair rate is of order $R \sim \frac{3}{2}\pi\alpha \simeq 0.03$. However, in practice the production rate is also reduced by the Bohr energy divided by the finite width of the beam energies, since only collisions in the energy window $\delta E \simeq$

$m_\mu \alpha^2/4$ are effective in producing bound states. For example, if the beam resolution is of order $\Delta E_\pm = 0.01m_\mu \sim 1$ MeV, the effective R is reduced by a further $\delta E/\Delta E_\pm \simeq 10^{-3}$, leading to a production of $(\mu^+ \mu^-)$ at $\sim 5 \times 10^{-5}$ of the standard $e^+e^- \rightarrow \ell^+ \ell^-$ rate.

Since the $(\mu^+ \mu^-)$ state in the FISR method is produced through a single $C = -$ photon, n^3S_1 states (and not n^1S_0) are produced, which decay almost always to e^\pm pairs, as illustrated in Fig. 2. Note that this holds even for radiative transitions through the sequences $n''^3S_1 \rightarrow n'P \rightarrow n^3S_1$, since the intermediate P states do not annihilate.

The $(\mu^+ \mu^-)$ bound states, once produced, can in principle be studied by exposure to $O(\text{ps})$ laser or microwave bursts, or dissociated into free μ^\pm by passing through a foil. Because of the novel kinematics of the FISR, the true muonium state can be produced within a laser cavity. For example, an intense laser source can conceivably excite the nS state of the atom to a P state before the former's annihilation decay. A $2P$ state produced in this way has a lifetime of 15.4 ps times dilation factor γ . In principle this allows precision spectroscopy of true muonium, including measurements of the $2P-2S$ and other splittings. Laser spectroscopy of (μZ) atoms is reviewed in Ref. [22].

In this Letter we also propose a second production mechanism, $e^+e^- \rightarrow \gamma(\mu^+ \mu^-)$, which can be used for high-energy colliding beams with conventional configuration. It has the advantage that the production rate is independent of beam resolution, and removes the $(\mu^+ \mu^-)$ completely from the beam line since the atom recoils against a coproduced hard γ . While the production of the real γ costs an additional factor of α in the rate, the kinematics is exceptionally clean: Since the process is quasi-two-body, the γ is nearly monochromatic [neglecting the $(\mu^+ \mu^-)$ binding energy] as a function of the total c.m. beam energy \sqrt{s} , $E_\gamma = (s - 4m_\mu^2)/2\sqrt{s}$. Furthermore, the $(\mu^+ \mu^-)$ lifetime is enhanced by the dilation factor $\gamma = (s + 4m_\mu^2)/4m_\mu \sqrt{s}$. The dominant Feynman diagrams for $e^+e^- \rightarrow \gamma(\ell^+ \ell^-)$ are shown in Fig. 3. If E_γ is large compared to m_μ , and its angle from the beam is large,

one can also have significant radiation from the μ lines. In fact, if the hard γ is emitted by a μ , the true muonium state is formed in the para n^1S_0 , $C = +$ state, which leads to two-photon annihilation decays. In this case both e^+e^- and $\gamma\gamma$ final states appear, accompanied by a decay gap.

The $O(\alpha^3)$ Born amplitude for the process $e^+e^- \rightarrow \gamma\mu^+\mu^-$ (free μ 's) in the kinematic regime $m_e^2/s, m_\mu^2/s \ll 1$ was first computed long ago in Ref. [23]. More recently, a related collaboration [24] specialized this calculation to precisely the desired kinematics: The invariant mass square s_1 of the μ^\pm pair is assumed small compared to the total c.m. squared energy s . In this case, the Born differential cross section for the diagrams in Fig. 3 is

$$d\sigma = \frac{\alpha^3(1+c^2)}{ss_1(1-c^2)}(2\delta + 1 - 2x_-x_+)dx_-dc ds_1, \quad (3)$$

where c is defined as the cosine of the angle between the e^- and μ^- [and hence also the $(\mu^+ \mu^-)$ atom], $\delta \equiv m_\mu^2/s_1 \simeq \frac{1}{4}$ for $(\mu^+ \mu^-)$ bound states, x_\pm are the fractions of the half of the c.m. beam energy $E_\pm/(\sqrt{s}/2)$ that is carried by μ^\pm (the other half being carried by the γ) so that $x_+ + x_- = 1$, and the range of x_\pm is given by

$$\frac{1}{2}(1 - \beta') \leq x_\pm \leq \frac{1}{2}(1 + \beta'), \quad (4)$$

where $\beta' \equiv \sqrt{1 - 4\delta}$ is the velocity of either of the μ^\pm in their c.m. frame. In addition, the hard photon momentum makes an angle θ_γ with the initial e^- that is assumed to lie outside of narrow cones of opening angle θ_0 around the beam axis, $\theta_0 < \theta_\gamma < \pi - \theta_0$, where $2m_\mu/\sqrt{s} \ll \theta_0 \ll 1$. Note that the γ and $(\mu^+ \mu^-)$ are back to back, $\theta_\gamma = \pi - \theta$.

The differential cross section in Eq. (3) becomes singular when the γ [and hence also the $(\mu^+ \mu^-)$] is collinear with the beam. For the purpose of our cross section estimates, we integrate c over the range excluding the beam cone, $c \in [-c_0, c_0]$, where $c_0 \equiv \cos\theta_0$. Using also Eq. (4) to integrate over x_- , one obtains

$$\frac{d\sigma}{ds_1} = 2\beta' \left[\ln\left(\frac{1+c_0}{1-c_0}\right) - c_0 \right] \frac{\alpha^3}{ss_1}. \quad (5)$$

The factor β' , indicating that the cross section vanishes at μ^\pm threshold, arises simply from three-body phase space.

Equations (3) and (5) describe a process in which the μ^\pm pair carry an invariant mass s_1 small compared to s , but are not necessarily bound together. In order to compute the cross section for such a process, one must again include the SSS threshold Coulomb resummation factor [19]. Here the β' in Eq. (5) refers to the (continuous) velocity of each of a free μ^\pm pair in its c.m. frame, whereas β' in the bound-state formalism refers to the (quantized) velocity of each particle within their Coulomb potential well. Nevertheless, as argued in the previous case, by duality the same cross

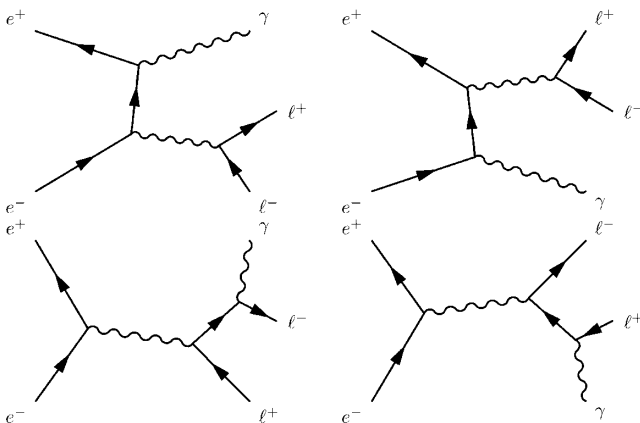


FIG. 3. Dominant Feynman diagrams for $e^+e^- \rightarrow \gamma(\ell^+ \ell^-)$.

section formulas still hold in the bound-state regime if the SSS factor is taken into account and the weights of the discrete transitions are properly included and smeared over the allowed energy range for bound states [18]. One then obtains

$$\frac{d\sigma}{ds_1} = 2\pi \left[\ln \left(\frac{1+c_0}{1-c_0} \right) - c_0 \right] \frac{\alpha^4}{ss_1}. \quad (6)$$

The relevant range of ds_1 is just that where bound Bohr states occur, which begin at energy $\alpha^2 m_\mu/4$ below the pair creation threshold $s_1 = 4m_\mu^2$, and thus give rise to $ds_1 \approx m_\mu^2 \alpha^2$. Thus one obtains

$$\sigma \approx \frac{\pi}{2} \left[\ln \left(\frac{1+c_0}{1-c_0} \right) - c_0 \right] \frac{\alpha^6}{s}. \quad (7)$$

The angular factor is again singular for $c_0 = \pm 1$, varying from zero at $\theta_0 = \pi/2$, to unity near $\pi/4$, to over 7 at 2° .

Note that $\beta \equiv \sqrt{1 - 4m_\mu^2/s}$ differs from β' used for $e^+e^- \rightarrow \gamma(\mu^+\mu^-)$; for processes $e^+e^- \rightarrow \gamma(\mu^+\mu^-)$ with the same value of s for which Eq. (3) and following are applicable, recall that $m_\mu^2 \ll s$ and hence $\beta \approx 1$. The ratio $\sigma[e^+e^- \rightarrow \gamma(\mu^+\mu^-)]/\sigma(e^+e^- \rightarrow \mu^+\mu^-)$ at the same value of s is therefore just a number close to unity (e.g., 2.66 for $\theta_0 = 2^\circ$) times α^4 . While this $O(10^{-8})$ suppression may seem overwhelming, it is within the capabilities of modern e^+e^- facilities. For example, the BEPCII peak luminosity will be $10^{33} \text{ cm}^{-2} \text{ s}^{-1}$ at a c.m. energy of 3.78 GeV, but varying between 2 and 4.6 GeV [25]. At 2 GeV about 5 events $e^+e^- \rightarrow \gamma(\mu^+\mu^-)$ occur per year of run time, and the yield increases with $1/s$. On the other hand, for smaller values of s the dilation factor γ for $(\mu^+\mu^-)$ becomes shorter, thus diminishing its lifetime and hence track length.

The production is much more prominent if one performs a cut on s_1 values near the μ^\pm threshold $4m_\mu^2$. In that case one should compare Eq. (5) to the derivative $d\sigma(e^+e^- \rightarrow \mu^+\mu^-)/ds$ [which is not actually a differential cross section but rather the difference of $\sigma(e^+e^- \rightarrow \mu^+\mu^-)$ between bins at c.m. squared energies s and $s + ds$]. Then the relative suppression is only $O(\alpha^2)$, one α arising from the extra photon and one from the SSS factor.

Between the two proposals presented here, $e^+e^- \rightarrow (\mu^+\mu^-)$ with beams merging at a small crossing angle, and the rarer process $e^+e^- \rightarrow \gamma(\mu^+\mu^-)$ that can access both ortho and para states with conventional beam kinematics, the discovery and observation of the true muonium atom $(\mu^+\mu^-)$ appears to be well within current experimental capabilities.

This research was supported under DOE Contract No. DE-AC02-76SF00515 (S.J.B.) and NSF Grant No. PHY-0757394 (R.F.L.). S.J.B. thanks Spencer Klein and Mike Woods for useful conversations, and R.F.L.

thanks the SLAC Theory Group, where this work was inspired, for their hospitality.

*sjbth@slac.stanford.edu

†Richard.Lebed@asu.edu

- [1] R. E. Marshak and H. A. Bethe, Phys. Rev. **72**, 506 (1947); C. M. G. Lattes, H. Muirhead, G. P. S. Occhialini, and C. F. Powell, Nature (London) **159**, 694 (1947); **160**, 453 (1947); **160**, 486 (1947).
- [2] J. Pirenne, Arch. Sci. Phys. Nat. **28**, 233 (1946).
- [3] M. Deutsch, Phys. Rev. **82**, 455 (1951).
- [4] J. I. Friedman and V. L. Telegdi, Phys. Rev. **105**, 1681 (1957).
- [5] V. W. Hughes, D. W. McColm, K. Ziock, and R. Prepost, Phys. Rev. Lett. **5**, 63 (1960).
- [6] S. Bilen'kii, N. van Hieu, L. Nemenov, and F. Tkebuchava, Sov. J. Nucl. Phys. **10**, 469 (1969).
- [7] V. W. Hughes and B. Maglic, Bull. Am. Phys. Soc. **16**, 65 (1971).
- [8] J. Malenfant, Phys. Rev. D **36**, 863 (1987).
- [9] S. G. Karshenboim, U. D. Jentschura, V. G. Ivanov, and G. Soff, Phys. Lett. B **424**, 397 (1998).
- [10] R. Coombes *et al.*, Phys. Rev. Lett. **37**, 249 (1976).
- [11] D. B. Cassidy and A. P. Mills, Nature (London) **449**, 195 (2007).
- [12] E. Holvik and H. A. Olsen, Phys. Rev. D **35**, 2124 (1987); N. Arteaga-Romero, C. Carimalo, and V. G. Serbo, Phys. Rev. A **62**, 032501 (2000).
- [13] I. F. Ginzburg, U. D. Jentschura, S. G. Karshenboim, F. Krauss, V. G. Serbo, and G. Soff, Phys. Rev. C **58**, 3565 (1998).
- [14] L. Nemenov, Yad. Fiz. **15**, 1047 (1972) [Sov. J. Nucl. Phys. **15**, 582 (1972)]; G. A. Kozlov, Yad. Fiz. **48**, 265 (1988) [Sov. J. Nucl. Phys. **48**, 167 (1988)].
- [15] J. W. Moffat, Phys. Rev. Lett. **35**, 1605 (1975).
- [16] D. A. Owen and W. W. Repko, Phys. Rev. A **5**, 1570 (1972).
- [17] U. D. Jentschura, G. Soff, V. G. Ivanov, and S. G. Karshenboim, Phys. Lett. B **424**, 397 (1998); Phys. Rev. A **56**, 4483 (1997); S. G. Karshenboim, V. G. Ivanov, U. D. Jentschura, and G. Soff, Zh. Eksp. Teor. Fiz. **113**, 409 (1998) [J. Exp. Theor. Phys. **86**, 226 (1998)].
- [18] J. D. Bjorken (private communication).
- [19] A. Sommerfeld, *Atombau und Spektrallinien* (Vieweg, Braunschweig, 1939), Vol. II; A. D. Sakharov, Sov. Phys. JETP **18**, 631 (1948); J. Schwinger, *Particles, Sources, and Fields* (Perseus, New York, 1998), Vol. 2.
- [20] M. Mizushima, *Quantum Mechanics of Atomic Spectra and Atomic Structure* (Benjamin, New York, 1970).
- [21] J. D. Bjorken, Lect. Notes Phys. **56**, 93 (1976).
- [22] K. Jungmann, Z. Phys. C **56**, S59 (1992).
- [23] E. A. Kuraev and G. V. Meledin, Nucl. Phys. **B122**, 485 (1977).
- [24] A. B. Arbuzov, E. Bartos, V. V. Bytev, E. A. Kuraev, and Z. K. Silagadze, Pis'ma Zh. Eksp. Teor. Fiz. **80**, 806 (2004) [JETP Lett. **80**, 678 (2004)].
- [25] F. A. Harris (BES Collaboration), Int. J. Mod. Phys. A **24**, 377 (2009).